
USING MONTE CARLO TREE SEARCH TO CALCULATE MUTUAL INFORMATION IN HIGH DIMENSIONS

Nick Carrara
Physics Department
University of California, Davis
Davis, CA 95616
nmcarrara@ucdavis.edu

Jesse Ernst
Physics Department
University at Albany, SUNY
Albany, NY 12222
jae@albany.edu

ABSTRACT

Mutual information is an important measure of the dependence among variables. It has become widely used in statistics, machine learning, biology, etc. However, the standard techniques for estimating it often perform poorly in higher dimensions or with noisy variables. Here we significantly improve one of the standard methods for calculating mutual information by combining it with a modified Monte Carlo Tree Search. We present results which show that our method gives accurate results where the standard methods fail. We also describe the software implementation of our method and give details on the publicly-available code.

1 Introduction

Mutual information (MI) [1] is widely used to quantify the strength of the relationship among variables. In a simple case, if a set of elements is characterized by two variables V_1 and V_2 , then it is the amount by which knowing the values of V_1 for the objects reduces the entropy in the values of V_2 . Informally, MI measures how much the values of V_1 reveal about the values of V_2 . As expected, it is symmetric: $I[V_1; V_2] = I[V_2; V_1]$.

MI is more broadly useful than the correlation coefficient [1, 2] because while the correlation coefficient assumes a linear relationship between the variables, MI measures the strength of the relationship without any assumption about its underlying functional form. MI is particularly useful within machine learning (ML) applications as one typically has a large number of variables with complex relationships among them. Further, one generally has samples from the parent distributions, not the distributions themselves, and so the functional relationships among the variables are unknowable.

Throughout this paper, we will focus primarily on a standard *binary classification problem*. Here, one has elements (*events*) that belong to one of two classes (*signal* and *background*), and for each event one has the values for a set of variables (called features or discriminating variables) for estimating the event's class. In practice, a set of features is often used as input to a neural network or other classification algorithm to estimate an event's class.

MI is important in judging the discriminating power of features because the MI between the event class and the feature is the amount by which knowing the value of a feature reduces the entropy of the class. Or, informally: How well can the values of the feature predict the class? Measuring the MI between features and class values is often used to choose the most effective features; a process known as feature selection [3, 4, 5, 6, 7]. The most common procedure is to simply rank features based on the MI between their values and the class values [8, 9, 10, 11]. There are also various heuristics for judging groups of variables [12, 10, 13, 14, 15], although these become intractable as the number of dimensions grows.

In an earlier paper, we emphasized that the MI between all available features and the class values (if one can measure it accurately), gives a useful estimate of the upper limit of separability between the classes [16]. That is, it quantifies how well any algorithm that uses all of those features as input can ever perform as a classifier. Equivalently, it can be viewed as quantifying how much, if any, discriminating information from the features was lost by the transformation that used them, a quantity which we call Δ_{TI} .

While extremely useful for problems with a small number of variables, MI is less useful as the number of variables grows because the methods for estimating it rapidly become unreliable with increasing dimension. And unfortunately, that is the situation in a wide range of class-separation problems [17]. The most widely used method for calculating MI was introduced by Kraskov et al. (KSG) [18], but even with only a few dimensions, it can significantly underestimate MI if variables are noisy and/or have significant correlations among them. It has been noted that in these cases, KSG and similar techniques are more useful for identifying the presence or absence of correlations than they are for actually finding an accurate value of MI [19, 20]. This greatly limits MI’s usefulness for setting a limit on class separability [16], or for feature selection. In this work, we describe a method we developed, based on KSG, that allows us to accurately estimate MI in higher dimensions, in the presence of noise, and in the presence of correlations among variables.

In high dimensions and in the presence of noise and/or strong dependence among variables, KSG’s estimate of MI is known to fall significantly below the true value [21, 22]. One could in principle remedy this by somehow choosing a subset of variables, or transformations of them, such that each variable would have independent information about the class values. The remaining variables, which have no independent information about the event class, would then be discarded. Note that if one included these discarded variables in the calculation, the true value of MI would not change, but KSG’s estimate of MI would be falsely low. Alternatively, one could test all subsets of variables to find the subset with the largest KSG estimate of MI. Unfortunately, either of these brute-force approaches would quickly become intractable for more than a few dimensions.

Our approach is to efficiently search for the subset of variables with the largest returned MI value from KSG. We do this by recasting the problem of choosing included/excluded variables into the problem of searching the tree of possible moves in turn-based strategy games. This will allow us to use the Monte Carlo Tree Search method (MCTS) [23] which was developed specifically to improve computers’ ability to play these games by allowing them to search a decision tree for the optimum move without doing a brute-force evaluation of every possible path from the current state of the game to its conclusion [24]. Our approach therefore, is to: 1) recast the problem of searching for the optimum set of variables into a problem that is similar to turn-based games, and then 2) modify the MCTS method so that it can quickly find the set of variables that maximizes KSG’s estimate of MI.

1.1 Organization

In Section 2 we briefly review MI and several related quantities. We also discuss MI’s connection to the upper limit of separability between event classes and to the lower limit on classification error rates. We also discuss MI’s importance in the closely related problem of feature selection. In Sections 3 and 4 we review the standard methods for estimating MI, and the problems they have in high dimensions. In Section 5 we discuss how we use a modified MCTS method in combination with KSG to estimate MI even in high dimensions and in the presence of noisy variables and give some details on our software implementation and on how to access the publicly-available code. In Section 6 we compare the results of our method to those of standard methods. The conclusion (Section 7) includes a glossary of the most used terms and acronyms,

2 Mutual Information, Separability, and Classification Errors

Mutual information (MI) is a robust measure of the dependence among variables. Because it characterizes both linear and non-linear dependencies among variables and is also invariant under smooth and uniquely invertible transformations of variables, it has become a centrally important data analysis tool in a wide range of fields from machine learning, epidemiology, domain generation, deep learning, biology, etc. [25, 26, 27, 28].

The definition of MI follows directly from the basic building block of information theory: Shannon Entropy, or H [29]. For a random discrete variable $x_i \in X$,

$$H[X] = - \sum_{i=1}^{|X|} p(x_i) \log p(x_i) \quad (1)$$

describes the uncertainty in X , or equivalently, the amount of information per element that one would need to perfectly predict the values of X . If one has two variables, the related quantity

$$H[X|Y] = - \sum_{j=1}^{|Y|} p(y_j) \sum_{i=1}^{|X|} p(x_i|y_j) \log p(x_i|y_j) \quad (2)$$

is the conditional entropy and is the amount of entropy, or uncertainty, remaining in the values of X after one is given the values of Y . The mutual information $I[X; Y]$ of X and Y , is then defined in a straightforward way as the amount by which the entropy of Y is reduced by knowing the values of X , or vice versa. Thus,

$$I[X; Y] = I[Y; X] = H[Y] - H[Y|X] = H[X] - H[X|Y] \quad (3)$$

and quantifies the amount that the values of X tell you about the values of Y . We use base-2 for logarithms throughout, which gives H and I the units of bits.

In a typical binary classification problem, where one uses X to estimate Y , these quantities are particularly simple. For each event, X may be single-valued or multi-dimensional, but Y has one of only two values. Thus, if the population of events is equally distributed between the two classes, then $H[Y] = 1$ and $I[X; Y] = 1 - H[Y|X]$.

For the binary classification problem, $I[X; Y]$ is equivalent to the Jensen-Shannon divergence (JSD) between the X distributions for the two classes of events. Intuitively, a larger difference between the X -distribution for signal and the X -distribution for background corresponds to X revealing more about the event class Y .

2.1 The Upper Limit of Separability

In a previous paper [16], we pointed out that if one can accurately measure MI in a multidimensional space, then its value and an appeal to the Data Processing Inequality (DPI) [1] allow one to: 1) set a testable upper-limit on the separability between classes of events in a binary classification problem, and 2) more rapidly find a set of discriminating variables.

As a reminder, the Data Processing Inequality (DPI) formalizes the intuitive notion that an algorithm using X to predict Y can not reduce the entropy of Y below some fundamental amount of information that the values of X hold about the values of Y . That fundamental amount is the MI between X and Y . That the DPI is an inequality rather than an equality reflects the fact that an unwise use of the values of X for predicting the values of Y could discard information. An extreme example would be a function that casts all values of X into a single value, resulting in the loss of all information that X could have revealed about Y . For smooth invertible functions of X , the equality will hold.

Combining an accurate measurement of MI with the DPI allows one to set an upper-limit on class separability and then use it to objectively check the effectiveness of any discriminating algorithm. In a standard binary classification problem, one has a vector of discriminating variables $x \in X$ for each event, and then uses an ML algorithm to combine them into a single value $f(x)$ which estimates the class value $y \in Y$. Using these to objectively test an algorithm is straightforward: 1) Compute $I[X; Y]$, which we refer to as I_{initial} or I_i . I_i is the information that the vectors of discriminating variables X can reveal about the class values Y . 2) Use the X values in a discriminating algorithm to produce output values $f(X)$ that predict the event classes Y . 3) Compute $I[f(X); Y]$, which we refer to as I_{final} or I_f . I_f is the information that the algorithm output values $f(X)$ can reveal about the class values Y . According to the DPI, $I[f(X); Y] \leq I[X; Y]$ (i.e., $I_f \leq I_i$) where the equality holds only if the algorithm is optimal and has not discarded any information that X could have revealed about Y . $I_i - I_f$, which we define as $\Delta_{\mathcal{T}I}$, is the information loss caused by the transform. For a classification model, it is the average number of bits of information per event that the model has lost.

$\Delta_{\mathcal{T}I}$ is an objective way to judge whether a classification algorithm is optimum. This approach is very different from the usual practice of assuming that a classification algorithm is optimum when neither additional training nor alternate algorithms seem to improve a figure of merit. Less than optimal results ($\Delta_{\mathcal{T}I} > 0$) can occur when, for example, an algorithm settles into a local minimum, when it has too few free parameters to fully model the space of the input vectors x , or when the algorithm is poorly suited to the problem.

An accurate value of I_i is also valuable on its own as a metric for choosing discriminating variables (feature selection) [9, 30, 31]. Feature selection has numerous heuristic procedures involving adding or dropping variables and then, after each change: 1) retraining the algorithm, 2) reprocessing the events through the algorithm, and 3) measuring the change in some figure of merit. These ad-hoc approaches are needed because a brute-force comparison of all possible combinations of potential discriminating variables is generally intractable. There is no perfect non-brute-force solution to this problem, but if one can quickly and accurately compute I_i , then one can rapidly compare sets of potential features without ever training an ML model on them. As we discuss below, we have been able to compute I_i roughly two orders of magnitude faster than training and testing an ML model, and hence potential sets of features can be evaluated extremely quickly.

Note that comparing $I[X; Y]$ to $I[f(X); Y]$ where Y is discrete, as described above, differs from the Infomax strategy [32, 33], where one uses $I[X; f(X)]$, where both X and $f(X)$ are continuous distributions. With Infomax, as $f(x)$ is developed, one uses the differential (continuous) entropy $I[X; f(X)]$ as a figure of merit to minimize the amount of information lost as X is transformed into $f(x)$. Rather than following Infomax, we take advantage of the fact

that our problem has discrete answers. This lets us compare the discrete Shannon entropies $I[X; Y]$ and $I[f(X); Y]$. That comparison allows us to quantify absolutely the effectiveness of a classifier, and quantify absolutely the usefulness of potential discriminating features.

The challenge in using I_i for feature selection or $\Delta_T I$ for quantitatively judging a model, is in accurately measuring I_i . While calculating I_f is simple because both the algorithm output $f(X)$ and the class values Y are generally one dimensional, calculating I_i is much more difficult because the dimension of the X vectors is equal to the number of discriminating variables, which is often large. And all current standard methods for computing MI struggle in high dimensions. Thus much of the rest of this paper will focus on accurately computing I_i .

2.2 Figures of Merit

Before continuing with the calculation of I_i , it is worth briefly discussing MI as a figure of merit (FOM). MI is defined clearly as the amount by which the entropy of one variable is reduced by knowing the value of another variable (or set of variables). In the discussion above, we call an algorithm optimum if $\Delta_T I = 0$, and thus its output has as many bits of information about the class label as the original variables had. And we compare two potential sets of discriminating variables by comparing how many bits of information they hold about the class label. But for a particular problem, other FOM's may be preferred [34]. Examples include: the largest expected statistical significance, the smallest error rate, the smallest false-positive rate within some constraint on the false-negative rate, etc. These will all tend to improve with improving MI, but it isn't generally possible to directly convert from one FOM to another.

The relationship between error rate and MI has been studied extensively. For a given $I[X; Y]$, the lower bound and upper bound on the error rate for Y are given by Fano's limit [1, 35] and the Hellman-Raviv limit [36] respectively. Fano's limit states that for a given MI, no algorithm can be found with an error rate lower than $P_e > H^{-1}(1 - I[X; Y])$, where H^{-1} is the inverse of the Shannon entropy. The Hellman-Raviv limit states that it is always possible to find an algorithm with an error rate better than $H(1 - I[X; Y])/2$. These are shown in figure 1.

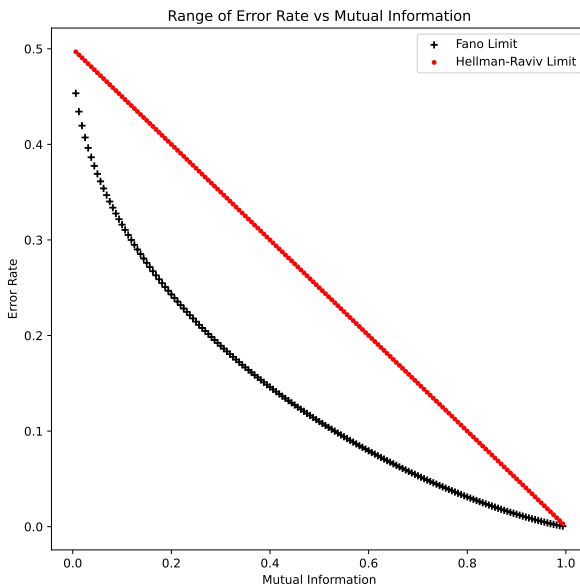


Figure 1: Fano and Hellman-Raviv limits on error-rate versus MI in bits for a binary classifier. The two curves define the lower and upper bounds respectively on the error rate, P_e , as a function of MI for any classifier, i.e. $H(1 - I[X; Y])/2 > P_e > H^{-1}(1 - I[X; Y])$.

Note that both limiting cases make sense. In the limit where $MI=0$ and thus X gives no information about Y , all algorithms will have a 50% error rate. In the limit of $MI=1$, X gives complete information about Y and it is always possible to find an algorithm with a 0% error rate. Between these two cases, there is a range of possible error-rates for a given MI.

Using Δ_{TI} to decide whether an algorithm is optimum remains valid, independent of one's choice of FOM. An algorithm that discards information ($\Delta_{TI} > 0$) will have a lower (or at least not better) FOM than one with ($\Delta_{TI} = 0$) for any reasonable FOM. Using I_i for feature selection is more subtle. Using I_i guarantees that the output from an optimum algorithm will have the largest possible MI with the class label, but figure 1 shows that there will be a range of corresponding error rates. So in principle, it might be possible to choose a set of variables with lower I_i but which nonetheless has a smaller error rate. We suspect that this will be uncommon, but see no way to prove it. It likely depends on details of the distributions, and we don't consider it further

3 MI Estimators

While widely useful, MI is notoriously difficult to compute. The fundamental problem is that one generally doesn't have closed functional forms for $p(x|y)$, $p(x)$, or $p(y)$ but rather has finite i.i.d. samples drawn from them $z_i = (x_i, y_i) \in \mathcal{Z}$, $i = 1, \dots, N$, requiring the use of numerical methods for integration. The calligraphic symbols $\mathcal{X} \subset X$ are used to denote sample distributions (point sets) drawn from the underlying space X .

3.1 Histogram Methods

The simplest approach for computing MI from i.i.d. samples is to create a histogram for the three sample distributions \mathcal{X} , \mathcal{Y} , and $\mathcal{Z} = \mathcal{X} \times \mathcal{Y}$ by choosing some suitable binning such that each space is partitioned into $h_{\mathcal{X}}$, $h_{\mathcal{Y}}$ and $h_{\mathcal{Z}} = h_{\mathcal{X}}h_{\mathcal{Y}}$ bins. The value of the probability in each bin is simply given by the number of points which land in that bin relative to the others, i.e. $P_x(i) \approx n_x(i)/N$, $P_y(j) \approx n_y(j)/N$ and $P_z(i, j) \approx n_z(i, j)/N$ where $i = 1, \dots, h_{\mathcal{X}}$ and $j = 1, \dots, h_{\mathcal{Y}}$. The MI is approximated by the sum,

$$I[\mathcal{X}; \mathcal{Y}] \approx \sum_{i,j} P_z(i, j) \log \frac{P_z(i, j)}{P_x(i)P_y(j)}. \quad (4)$$

While the histogram method converges to the true MI in the limit of $N \rightarrow \infty$ and bin sizes going to zero, it becomes intractable as the dimension of the spaces increases.

As discussed by KSG, methods for computing MI based on cumulant expansions or entropy maximization [37, 38], have poor accuracy. Methods based on kernel density estimators (KDE) can do well in limited circumstances, but often perform no better than a linear correlation coefficient¹.

3.2 Non-parametric Entropy Estimators

The non-parametric estimators described here are a family of k -nearest neighbor (k NN) methods, which estimate the local density at each point in $z_i = (x_i, y_i)$, $x_i \in \mathcal{X} \subset X$ and $y_i \in \mathcal{Y} \subset Y$ by using information from its k -nearest neighbors. The first goal is to construct an unbiased estimator of the Shannon entropy $H[X]$, which has the form

$$\hat{H}[X] = -\frac{1}{N} \sum_{i=1}^N \log p(x_i), \quad (5)$$

where $p(x_i)$ is the *true* density at x_i so that \hat{H} converges to the *true* entropy as $N \rightarrow \infty^2$.

3.2.1 KL Estimator

The KSG algorithm for estimating MI is based on an approach developed by L.F. Kozachenko and N.N. Leonenko (KL) for estimating the Shannon entropy $H[X]$ of a continuous variable $x \in X$ [41]. We will reproduce the derivation here, which begins by writing the probability that the k th-nearest neighbor of the point $x_i \in \mathcal{X}$ exists in a small spherical shell of radius $\varepsilon/2$ and thickness $d\varepsilon$ so that there are $k - 1$ points lying within the shell at points $r_i < \varepsilon/2$ and that there are $N - k - 1$ points lying at distances $r_i > \varepsilon/2 + d\varepsilon$. This distribution is given by the multinomial,

$$P_{\varepsilon}(x_i)d\varepsilon = \frac{N!}{1!(k-1)!(N-k-1)!} \times p_i^{k-1}(1-p_i)^{N-k-1} \frac{dp_i}{d\varepsilon} d\varepsilon, \quad (6)$$

¹See Section IV.A in [18]

²It is apparently provably impossible to find an unbiased method [39, 40]

where p_i is the probability mass integrated over the inner spherical region,

$$p_i = \int_{r_i < \varepsilon/2} dx p(x), \quad (7)$$

and where $p(x)$ is the *true* probability density. The distribution in (6) has the interesting property,

$$\langle \log p_i \rangle = \int d\varepsilon P_\varepsilon(x_i) \log p_i = \psi(k) - \psi(N), \quad (8)$$

where ψ is the digamma function ($\psi(x) = \Gamma(x)^{-1} d\Gamma(x)/dx$)³, and N is the number of points in the data set.

KL density assumption — The main assumption for all estimators comes from the next step, in which one assumes some form of the local density $p(x_i)$ in order to approximate p_i for each point. For the KL-estimator, and later the KSG estimator we assume that the local density around each point x_i is uniform (i.e. the density $p(x_i)$ does not vary much in the $\varepsilon/2$ ball),

$$p_i \approx c_d \varepsilon^d p(x_i), \quad (9)$$

where c_d is the volume of the unit ball in d -dimensions and ε is the distance to the k -neighbor. As we will see in the next section, it is more convenient to use rectangular volumes which are aligned with the coordinate axes of X and Y when defining the volumes of the p_i 's. In this coordinate system, the form of eq. (9) changes slightly to

$$p_i \approx \left(\prod_{m=1}^d \varepsilon_m^i \right) p(x_i), \quad (10)$$

where ε_m^i is some distance along the m th-dimension for the i th point. Using this form, we have from eq. (8)

$$\psi(k) - \psi(N) = \sum_{m=1}^d \langle \log \varepsilon_m^i \rangle + \langle \log p(x_i) \rangle. \quad (11)$$

Inserting the above into the unbiased estimator (5), one arrives at the KL entropy estimator, which contains a single parameter k ,

$$\hat{H}_{KL}^k[X] = -\psi(k) + \psi(N) + \frac{1}{N} \sum_{i=1}^N \sum_{m=1}^d \log(\varepsilon_m^i), \quad (12)$$

3.2.2 KSG Estimator

To extend the KL algorithm to estimate MI, one could naively plug in eq. (12) to the MI decomposition in eq. (3), which amounts to estimating the entropy of $\hat{H}[X]$, $\hat{H}[Y]$ and $\hat{H}[X \times Y]$ and combining them to give the MI,

$$\hat{I}_{\text{naive}}[X; Y] = \hat{H}[X] + \hat{H}[Y] - \hat{H}[X \times Y]. \quad (13)$$

However, as KSG point out in motivating their estimator, this can result in a bias from applying the KL estimator with the same parameter k to spaces of different dimension and scale, which leads to non-cancellation of the errors in the three entropy estimates⁴. One can see this by first applying the KL estimator to the joint space $X \times Y$,

$$\begin{aligned} \hat{H}_{KL}[X \times Y] &= -\psi(k_Z) + \psi(N) \\ &+ \frac{1}{N} \sum_{i=1}^N \sum_{m_Z=1}^{d_X+d_Y} \log(\varepsilon_{m_Z}^i), \end{aligned} \quad (14)$$

where $Z = X \times Y$. Plugging eq. (14) and the corresponding marginal estimates into eq. (13) we find,

$$\begin{aligned} \hat{I}_{\text{naive}}[X; Y] &= \psi(k_Z) + \psi(N) - \frac{1}{N} \sum_{i=1}^N \sum_{m_Z=1}^{d_X+d_Y} \log(\varepsilon_{m_Z}^i) \\ &- \psi(k_X) + \frac{1}{N} \sum_{i=1}^N \sum_{m_X=1}^{d_X} \log(\varepsilon_{m_X}^i) \\ &- \psi(k_Y) + \frac{1}{N} \sum_{i=1}^N \sum_{m_Y=1}^{d_Y} \log(\varepsilon_{m_Y}^i). \end{aligned} \quad (15)$$

³When x is discrete, the digamma function follows the recursion formula $\psi(x+1) = \psi(x) + 1/x$ and $\psi(1) = -C$ where $C = 0.5772156\dots$ is the Euler-Mascheroni constant. We can then easily compute $\psi(N) = \sum_{n=1}^{N-1} \frac{1}{n} - C$ for any integers N .

⁴See Section I page 2 of [18] for more discussion.

Mutual Information in High Dimensions

The nearest neighbor factors k_Z , k_X and k_Y are, in general, all different, and imposing $k_Z = k_X = k_Y$ can result in the volume terms $\langle \log \varepsilon_i \rangle$ not canceling and accumulating errors. KSG solves this problem by imposing that the volume measures used in the joint space Z is the same used in the marginal spaces X and Y .

KSG marginal assumption — Instead of choosing the same k for each space, they simply choose one $k = k_{X \times Y}$ for the joint space and then force the projected ε^i in each marginal space to be the same as in the joint space, i.e.

$$\sum_{m_Z=1}^{d_X+d_Y} \log(\varepsilon_{m_Z}^i) = \sum_{m_X=1}^{d_X} \log(\varepsilon_{m_X}^i) + \sum_{m_Y=1}^{d_Y} \log(\varepsilon_{m_Y}^i), \quad (16)$$

which simply amounts to adjusting the $\psi(k_X)$ and $\psi(k_Y)$ for each projected p_i in the marginal spaces. As noted by KSG, fixing k in the joint space requires the use of the L^∞ norm when defining p_i , which results in all distances being the same, i.e., $\varepsilon_m^i = \varepsilon^i$.

With the above adjustment, the functional form for the KSG estimator is

$$\hat{I}_{KSG}[X; Y] = \psi(k) + \psi(N) - \langle \psi(n_X + 1) \rangle - \langle \psi(n_Y + 1) \rangle, \quad (17)$$

where n_x is the number of points falling in the projected p_i and $\langle \psi(n_x + 1) \rangle$ is the mean over all points.

4 KSG: Limitations and Improvements

While the KSG estimator in eq. (17) works well in some applications, it is well known to consistently underestimate MI as noise and/or number of dimensions increases. Czyz et al. [22] have studied a wide range of MI estimators applied to forty different datasets with varying noise levels and numbers of dimensions. Of the 40 tests, KSG is accurate in 17 tests, underestimates MI (often significantly) in 23 tests, and overestimates MI in zero tests. Similarly, when introducing their G-KSG method, Marx and Fischer [42] show that over a wide range of datasets and dimensions, that the standard KSG method is either accurate or underestimates MI. That KSG consistently underestimates rather than overestimates MI when noise variables are added or as the data become sparse is central to our method of improving it.

There are several assumptions used in the KL/KSG estimators that lead to common failure modes:

1. **KSG marginal projections** - The central feature of the KSG estimator is that equation (16) is imposed when calculating the marginal entropies $\hat{H}[X]$ and $\hat{H}[Y]$. This feature is spoiled by the use of the naive estimator \hat{I}_{naive} in equation (13).
2. **Uniform local densities** - The single assumption of the KL estimator in approximating the probability mass in equation (9) is that the probability density $p(x_i)$ around the point $x_i \in \mathcal{X}$ is uniform. If this assumption is not satisfied, it can indirectly lead to the failure of the first assumption, since for arbitrary forms of the density estimate in equation (9) it is not immediately clear how to impose the cancellation of the resulting marginal volume terms. This problem occurs for several estimators based on KSG [20, 19] which we discuss in Section 4.2.
3. **Joint space L^∞ box** - KSG uses the L^∞ box to define ε_i and hence p_i in the joint space in eq. (16). This is not necessarily ideal for regions where the density is not uniform, as has been argued by several authors [19]. If this assumption is not satisfied, then, again, the first assumption will not be satisfied.
4. **Fixed k-neighbors** - A design choice of the KSG estimator and the KL estimator is to use a single k_Z value for all points $z_i \in \mathcal{Z}$ in the joint space. When densities have large variations in a space it may no longer be appropriate to use a fixed k value for all points. Unlike the other assumptions, choosing a dynamic k value does not spoil other KSG features.

4.1 Failure Modes of KSG

Most failure modes result from some aspect of the curse of dimensionality since, with any numerical method, we will be subject to limitations that come from sparseness. This has been explored in the case of KSG, to some extent by the original authors as well as others. Gao et al. [20] showed that the KSG estimator is consistent, but that its bias is dimension dependent and is of the order $\mathcal{O}(N^{-\frac{1}{d_x+d_y}})$.

In the original KSG paper [18], they show several examples comparing their estimator with closed functional forms of the MI for special distributions, and in each case where the estimate is meaningfully different from the true value, it is

Mutual Information in High Dimensions

an underestimate (see their figures 7, 10, 11, 12 and 14). Regions where MI is overestimated, which occurs when the number of samples is large, only gives a disagreement of a few percent.

While the remaining failure modes outlined below have several examples showing their effects, there are currently no quantitative explanations linking the behavior to the assumptions in the KSG estimator.

4.1.1 Redundant Variables

We define “redundant” variables as those which are dependent on other variables, but which do not introduce any new information. As a simple example, consider the case of two variables, X_1 and Y , where there exists correlations so that $p(x_1, y) = p(x_1)p(y|x_1)$ and $I[X_1; Y] > 0$ (i.e. $p(y|x_1) \neq p(y)$). Then, consider that with X_1 we add an additional variable $X_2 = f(X_1)$ which adds no new information about Y , but is highly correlated to X_1 , i.e.

$$\begin{aligned} p(x_1, y) \rightarrow p(x_1, x_2, y) &= p(x_1, x_2)p(y|x_1, x_2) \\ &= p(x_1, x_2)p(y|x_1). \end{aligned} \quad (18)$$

Then, the MI will remain invariant,

$$I[X_1; Y] \rightarrow I[X_1 \times f(X_1); Y] = I[X_1; Y]. \quad (19)$$

The authors have found that most situations involving redundant variables are handled well by KSG, as long as the number dimensions is small.

4.1.2 Noisy Variables

We define “noisy” variables as those that do not contain any additional information when added to a problem but are also independent of any other variables. Consider the example from the previous subsection except now where X_2 is independent of X_1 , i.e.

$$\begin{aligned} p(x_1, y) \rightarrow p(x_1, x_2, y) &= p(x_1, x_2)p(y|x_1, x_2) \\ &= p(x_1)p(x_2)p(y|x_1). \end{aligned} \quad (20)$$

Then, as it should be [43], the MI will also be invariant⁵,

$$I[X_1 \times X_2; Y] = I[X_1; Y]. \quad (21)$$

Because of the limitations of numerical methods variables with weak correlations may be difficult to distinguish from noisy variables. As with redundant variables, it is clear from numerous examples [44] that noisy variables cause KSG to underestimate MI.

4.1.3 Non-uniform PDF's

The KL estimator, and hence the KSG estimator, rely on the assumption in equation (9) that the local density $p(x_i)$ inside the ball p_i is uniform. As shown by several authors [19, 45] this assumption can lead to underestimation of MI in cases where the density varies largely over regions of the space. It is especially evident in regions around the boundary of a space, where the L^∞ box can extend into regions where the probability density goes to zero. Although the authors present some interesting solutions, we do not pursue them here.

4.1.4 Discontinuous Transformations

If one uses KSG to measure the MI between a set of variables and the event classes, and then applies a non-homeomorphic transformation to the variables, KSG will fail to find the same value of MI.⁶

4.2 Attempts to Address KSG Failure Modes

Attempts to improve KSG fall into one of several categories:

⁵Note the difference to the redundant case in which $p(x_1, x_2) = p(x_1)p(x_2|x_1)$.

⁶We are unaware of any method for measuring MI that is stable under non-homeomorphic transformations. In the most extreme case, the data processing inequality tells us that a set of variables that contain information about event classes retain that information, in principle, after applying a cryptographic hash function to them. But there is clearly no known method that can indicate even that the transformed variables contain a non-zero amount of information about the event classes.

- **Local density corrections** - Some suggested improvements to KSG attempt to address the density assumption pitfalls (items ‘b’ and ‘c’) as outlined at the start of section 4. These adjustments are concerned with the assumptions in eqs. (9) and 10 which are replaced by some other method.
- **Dynamic k-nearest neighbors** - This type of adjustment changes the fixed k value with one that depends on the local environment around each point z_i . This involves some method for determining the k_i at each point.

As shown by Marx and Fischer [42], the spoiling of the L^∞ condition in eq.(10) causes MI to be overestimated, which is undesirable. Some examples of the *local density correction* are discussed below in Sections 4.2.1 and 4.2.2. An example of *dynamic k-nearest neighbors* is discussed in Section 4.2.3 and an approach using neural networks is discussed in Section 4.2.4.

4.2.1 Local Non-Uniform Correction (LNC)

As an attempted correction to KSG’s problem with using the L^∞ box, S. Gao et al. proposed the *local non-uniform correction* (LNC) technique [19]. This technique adjusts the unbiased estimator for MI by replacing the L^∞ volume in the joint space with a volume computed from a PCA analysis. The basic idea is the following: Consider a point x_i whose k th-neighbor is x_k . With the collection of $k + 1$ points including x_i, x_k and all points closer than x_k , construct the correlation matrix C_{ij} and find its eigenvectors. By then projecting each point along the maximal eigenvectors, we can find a PCA bounding box which is rotated and skewed with respect to the L^∞ box. The assumption in this case is that the rotated PCA box is a better representation of the region of uniform probability around x_i . Once each volume is found, the MI is given by

$$\hat{I}_{LNC} = \hat{I}_{KSG} - \frac{1}{N} \sum_{i=1}^N \log \frac{\bar{V}_i}{V_i}, \quad (22)$$

where \bar{V}_i is the PCA volume and V_i is the L^∞ volume. Such an estimator has shown to give vast improvement to the naive KSG method, however current results are limited to two dimensional problems. The reason for this is its inability to deal with redundant information. To see this, consider a two-dimensional problem in which the variables $X \times Y$ have some non-trivial correlations. If we add to X a redundant copy, $X \rightarrow X \times f(X)$, then the true value of MI will be unchanged. If one naively uses the LNC method, however, one will find that the MI increases. This is because the volumes \bar{V}_i will generally decrease when computed in the redundant scenario and hence the LNC correction term will generally increase [44].

4.2.2 Kernel Density Estimators

Gao et al. proposed a kNN density estimator [45], called the *Local Likelihood Density Estimator* (LLDE), which weights neighbors using parameterized Gaussian kernels whose bandwidths are determined by the nearest neighbors. The motivation for this construction was to correct the biases of estimators near boundary points of the underlying manifold. One can easily see that any naive KDE methods will underestimate the density near boundaries, since large parts of the sampling region can be outside the manifold. While not directly a modification to KSG, the authors showed improvements to vanilla KDE methods in simple cases. In the study by Marx and Fischer, they showed that the LLDE estimator can lead to a dramatic over-estimation of MI, which makes it undesirable for our purposes.

Lord et al. proposed a geometric kNN density estimator [46], called *Geodesic-KNN* (G-KNN), which uses ellipsoids fit with PCA to describe the local density rather than the Gaussians of the LLDE method and the L^∞ box of KSG. While they show some decent results for low-dimensional examples, the G-KNN method also tends to overestimate MI, particularly in high-dimensional cases as shown by Marx and Fischer [42].

4.2.3 Geodesic-KSG (G-KSG)

A. Marx and J. Fischer introduced an extension to KSG [42] which uses geodesic distances to determine the k -nearest neighbors to use for each point in the joint space $X \times Y$. This k -adaptive G-KSG method shows improvement over standard KSG in high-dimensions and where there are a large number of noisy variables. Their estimate (like KSG) typically underestimates MI.

The G-KSG method works by first performing a manifold learning task on the data through a Geodesic Forest (GF) algorithm, which is then used to compute local geodesic distances that are used in place of the standard L^1 distances assumed by KSG. The benefit of this approach is that it does not alter the assumptions of the KSG estimator.

4.2.4 Mutual Information Neural Estimation (MINE)

The MINE approach uses the DPI to estimate MI by first training a neural network, $f : X \rightarrow Y$, to learn a suitable lower dimensional representation of the input space. In this way, the value of $I_i = I[X; Y]$ is found by first fitting the function f , and then estimated as $I_f = I[f(X); Y]$. While this scheme can work in principle, it assumes that the fitting of the function f reaches an optimum, i.e., that the learning algorithm has found the global maximum so that $I_i = I_f$. However, since no calculation of I_i is performed it cannot be known whether the function f actually achieves the equality.

5 Combining MCTS and KSG

5.1 Overview

Here we give an overview of our modification to the Monte Carlo Tree Search (MCTS) method, and of how we combine it with the KSG estimator to measure MI in higher dimensions and in the presence of noise. This section gives only the details that are needed to understand the rest of the paper. Additional implementation details are given in Section 5.2.

5.1.1 Introduction to Monte Carlo Tree Search

The Monte Carlo Tree Search (MCTS) method is a widely used algorithm for estimating the optimum next move in a game by judiciously searching a small fraction of the game tree. The timeline of its continual development over the past ~ 30 years is well-documented in Table 1 of [23]. At any point in a game, a player has c_1 choices for their move, which results in their opponent having c_2 choices for their move (see Figure 2). This continues down the tree until the players reach one of the final states of the game, at which point a winner is determined. These final states are represented by leaf nodes at the bottom of the tree, and each corresponds to a unique and fully specified game from the starting point. In all but the simplest games, the size of the tree makes it intractable to search exhaustively for an optimum next move. To estimate the optimum move, the MCTS method builds and searches only the most profitable portion of the game tree by repeatedly generating and evaluating multiple paths through the tree, choosing its current path based on the success rates of previous paths.

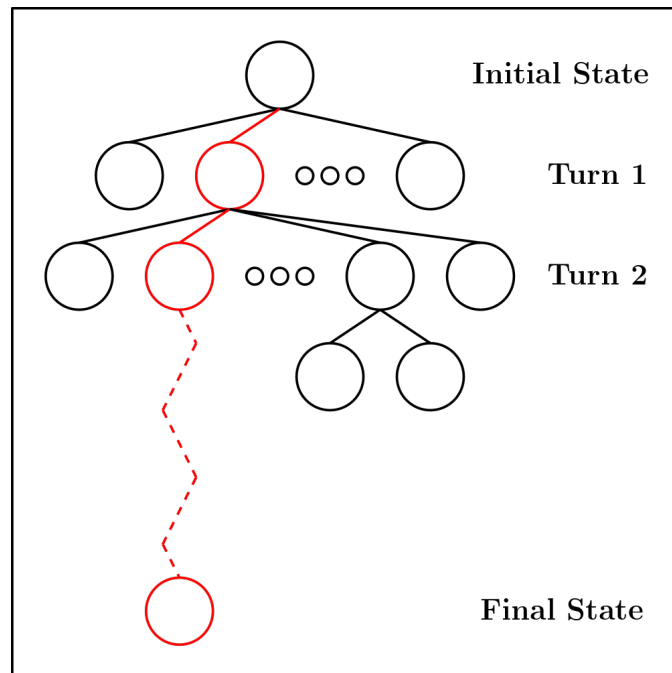


Figure 2: A search tree starts from an initial state, represented by the top node, and then branches according to the possible moves each player can choose. Each path through the tree represents a unique sequence of moves from the starting point to the end of the game.

The process begins from the top node, which represents the current state of the game. In the first stage, called *selection*, the forward steps are chosen based on the *tree policy* (see Figure 2). Among the previously explored nodes, the tree policy balances the benefit of stepping to a child node that has been successful in previous paths against the possibility that a lower performing node might, with more testing, ultimately be superior. The tension between these priorities is known as exploitation vs. exploration and its study has been central to the development of MCTS [23, 24, 47, 48]. Eventually the process will either reach the bottom of the tree (unlikely in realistic problems) or will reach a node that has at least one unexplored child node. At this point, the path will step to one of the unexplored child nodes. This stage is called *expansion*. Clearly all child nodes below this previously unexplored node will also be unexplored. Following expansion is the *simulation* stage, in which the rest of the path to the end of the tree is chosen by the *default policy* (often simply randomly) and the winner is recorded. This completion of the game using the default policy is called a *playout*. In the final stage, called *backpropagation*, the win/loss result becomes part of the statistics for all nodes that participated in that path. Those statistics, through the policy function, determine the next path through the tree. This process repeats until a sufficiently strong next move is found or a budgeted computing limit is reached. The MCTS method along with numerous variations is summarized in more detail elsewhere [23].

Central to the MCTS method is the tension between exploitation and exploration. There is an obvious benefit to further searching the portions of the tree with higher win rates to more accurately judge the best move. At the same time, the opportunity cost of that exploitation is that some other portion of the tree with potentially even better performance may be left unexplored. This idea appears in a broad range of statistical decision making problems and is usually framed as a slot machine with multiple arms (many-armed bandit). In this problem, a gambler has some number of trials in which to maximize their profit, and each arm has some unknown profitability distribution. The gambler wants to continue to pull an arm that has so far been successful, but at the same time wants to explore the possibility that some other less-tested arm might ultimately be even more profitable. The optimum balance between exploration and exploitation has been widely studied. A paper by Lai and Robbins [49] set a lower bound on the rate at which *regret*⁷ grows with the number of trials and thus created an absolute standard against which any decision policy could be measured. MCTS methods incorporate these results in the *tree policy* function, which is used to choose the next step forward among competing options.

5.1.2 T-KSG

KSG could be used to accurately measure MI from a dataset in high dimensions and with noisy variables if one had a way to first remove the noisy variables from KSG’s calculation. Because increasing noise and increasing sparsity cause KSG to underestimate MI, an equivalent goal is to find the subset of variables for which KSG gives the largest estimate of MI. Our approach (Tree-Search KSG, or T-KSG) is to use MCTS to efficiently search the power set of the input variables for the subset with the largest KSG-estimate of MI.

In our problem, we have n discriminating variables (i.e., x has dimension n) and so have 2^n unique sets of variables. We could in principle use KSG to measure MI for each of the 2^n possible sets of variables and use the largest value as our estimate of $I[X; Y]$. (We would use the largest value from among the subsets because: 1) sets that are missing variables with independent information about y will have their actual MI reduced by that amount of information, and 2) sets with redundant and/or noisy variables will have a lower estimate of MI for reasons discussed in Section 4.1.)

We can recast our problem as a decision tree by organizing the possible variable sets as shown in Figure 3. Beginning at the root node (level 1) with zero variables included in a set, one moves down the tree and chooses to include (exclude) variable one by stepping left (right). One continues stepping left (include) or right (exclude) at each layer until one reaches the bottom of the tree. Each leaf node then corresponds to unique set of included variables. Rather than an intractable search of the entire tree for the largest value of $I[X; Y]$, we will use some of the ideas from the MCTS technique to search only a portion of the tree.

The standard implementation of MCTS will not work for our problem. In MCTS, each path has a binary result (win/loss), while we have a continuous result (KSG’s estimate of $I[X; Y]$). Further, the reward for a path does not depend on the margin of victory, while we want to more strongly favor paths with a larger value for KSG-estimated MI. We modify MCTS in two significant ways: 1) We make an MCTS variation that uses a continuous result rather than a discrete result, and 2) To speed optimization, we close off (*gate*) sections of the search tree that perform poorly.

Discrete vs. Continuous: Standard MCTS records a binary (win/loss) result and back-propagates it up the tree, updating the statistics of the nodes that were part of the path. In our case, when we reach a leaf node, we use KSG to compute the MI of that path. That continuous result then needs to propagate up the tree and become part of the statistics for

⁷The regret of a procedure is the difference between its success and the success of an omniscient player who only ever pulls the optimum arm.

the tree¹⁰, 2) the mean MI and RMS values of MI when the node’s variable was included/excluded, and 3) the number of times that the MI of the path was within some fixed percentage of the highest recorded MI.

5.2.2 Tree Policy, Default Policy, and Gate Policy

- **Tree Policy** - In standard MCTS, the tree policy uses a multi-arm bandit function to choose the next step forward in a path based on the win/loss statistics of a node. In plain terms, for our tree with two options at each node, the tree policy creates competition between the include side and the exclude side of a node. If the node’s variable has independent information about the event class then paths that follow its include side will generally have higher MI, while if it is only noise, its exclude side will generally have higher MI, because KSG will underestimate MI when noise is included. As in standard MCTS, our modified multi-arm bandit function generally favors the higher-scoring side, but increasing weight is given to the side with fewer visits as the number of visits become more imbalanced. As with all multi-arm bandit functions, this is intended to optimize exploration vs. exploitation. In our variation, when the search arrives at a node, it chooses include vs. exclude by choosing the larger of $S_{inc} = P_{inc} + 4\sqrt{\log(n_{both}/n_{inc})}$ and $S_{exc} = P_{exc} + 4\sqrt{\log(n_{both}/n_{exc})}$, where P_{inc} (P_{exc}) is the percentage of paths through the include (exclude) side of the node that yield an MI within 5% of the maximum found MI, n_{both} is the total number of paths that have passed through either side of the node, and n_{inc} (n_{exc}) is the total number of paths that have passed through the include (exclude) side of the node.
- **Default Policy** - In standard MCTS, the default policy is applied when the search path reaches a node where none of its children has been explored. That of course also means that no children below that point have been explored. Here we can follow one of the standard approaches where one simply chooses randomly among the options until one reaches a leaf node at the bottom of the tree. In our case, that corresponds to choosing randomly whether to include/exclude all remaining variables. Then, as usual, that path is scored and its result propagated into the statistics of the nodes that were in the path.
- **Gate Policy** - In standard MCTS, all nodes in principle remain accessible to future paths. This causes significant problems for T-KSG. The issue is that when one includes noisy variables, the amount by which KSG will underestimate MI can vary widely. Unless one gradually removes variables that lower KSG’s estimate, converging to the highest estimate can be extremely slow.

To handle this problem, we introduce gates that permanently include (exclude) a variable that increases (decreases) MI more than one would expect from fluctuations. There is no equivalent to this in standard MCTS. Roughly, we permanently include a variable by first finding the percentage of paths that include the variable and have MI estimates that are in the top 10% of all paths. If a variable were neutral, one would of course expect to find 10% of its paths in the top 10%. If we find that it is more than 10% with confidence level of 3.5σ , then the variable is permanently included in future paths. Using the same standard, if paths that exclude the variable have higher MI estimates, then the variable will be permanently excluded.

5.2.3 Other Related MCTS Modifications

There are numerous MCTS variations, and hundreds of applications reported in the literature. We note two efforts that are somewhat similar to our work.

Gaudel and Sebag [51] study feature selection as a reinforcement learning problem, where the optimum feature set is the one with the smallest generalization error based on a reward with low computing cost. They additionally use MCTS to retain the features in the most often visited path of a feature-selection search tree. In contrast, our work focuses on using MCTS to calculate MI. An advantage of our approach is that calculating MI for a set of variables is extremely fast. As we discuss in section 2, knowing MI then lets us determine how well an ML algorithm could perform without ever actually creating one. Further, T-KSG will allow us to select approximately the smallest set of features that have this maximal MI value.

Chaudhry and Lee [52] study feature selection using, as we do, a binary include/exclude tree and searching it with MCTS. The resulting initial set of features will likely contain noisy along with useful features. They use a filtering technique to rank the best features in the set. This differs from our approach, as we measure MI for the entire feature set without using filtering methods that can potentially discard correlations among features.

¹⁰Note that the number of times a variable was included/excluded by a specific node is not the same as the number of times the variable was included/excluded in any path. More concretely, the number of times variable 5 was included when variable 3 was excluded is not the same as the total number of times variable 5 was ever included in any path.

6 Results

We compare MI measurements from standard KSG and from our tree-search modification of it (T-KSG) as the number of dimensions and the amount of noise increases. For each of the two tests below, we begin by making a baseline MI measurement using standard KSG ¹¹. We then begin adding noise and increasing the dimension of the variable space. We want the new noise variables to be similar to the existing data because added noise with, for example, a mean that is very different from the existing variables, would be easier to identify as noise. Thus, to create each noise variable, we randomly choose one of the existing variables, shuffle it, and then include the shuffled values back into in the data as a new variable. We repeat this process for each noise variable we add. The result is a dataset that has the original variables, which each contain some information about the class of each event, and some number of additional variables that give no information about event class. We can then compare the MI measurements from standard KSG to those from T-KSG in these noisy datasets.

6.1 Spherical Gaussian Test

For the first test, we use partially overlapping Gaussian distributions for signal and background and then add increasing amounts of noise. The signal data is a 5-dimensional Gaussian distribution with its center at $(0, 0, 0, 0, 0)$ and a diagonal covariance matrix with 1's along the diagonal. The background data have the same covariance matrix but are shifted to have their center at $(1, 1, 1, 1, 1)$. KSG's estimate of the MI for the data without any added noise is $\langle \text{MI} \rangle = 0.566 \pm 0.002$ bits. As discussed in footnote 11, we verified the accuracy of this baseline MI value.

We then added 6, 12, 25, 50, and finally 100 noise variables to the data, and the results are shown in Figure 4 and Table 1. Column one of Table 1 shows the amount of noise added. Column two shows the widely known problem that KSG rapidly begins to underestimate MI as noise and dimension increases. Column three, which is the key result, shows that T-KSG is able to maintain an accurate estimate of MI even as noise and the dimension of the dataset grows and becomes increasingly sparse ¹². Column four shows the number of noise variables that T-KSG included in its final/optimum path (i.e., its chosen set of variables), and it shows why T-KSG is so effective. Adding noise variables to KSG's input decreases its estimate of MI, and so as the T-KSG algorithm follows its procedure for finding the set of variables that maximizes MI, it will favor those paths that have fewer noise variables. Our T-KSG method could reasonably be viewed as simply a method to avoid passing noise into KSG.

Naively, one might expect T-KSG to reject all noise variables, which would correspond to all zeros in column four. That it can't is understandable by recognizing that for any optimization algorithm that calculates its FOM based on random sub-samples from a dataset, the FOM will have some statistical fluctuations even when it is at the optimum point. And so at that optimum point, the algorithm will be indifferent among options that are within that width. Looking at the first two entries in column two, one sees that, for this dataset, including as many as six noise variables reduces KSG's estimate of MI by only about 2%. Because this is within the range of fluctuations among different sub-samples, T-KSG is indifferent among paths that are within a few percent of one another.

Over many runs and a wide range of noise levels and dimensions, we found that T-KSG's optimum path consistently included all five good variables, excluded all but a few noise variables, and maintained an extremely accurate estimate of MI. This held even in the most extreme case of adding 100 noise variables to the five original variables – a space that would obviously be intractable to search via brute force.

6.2 SUSY Test

The Gaussian test of T-KSG in section 6.1 worked well, but we would like to test it on more realistic data. Here, we test T-KSG on a signal-background pair of data samples produced by Baldi, Sadowski, and Whiteson (BSW) [17] for their study on the use of deep-learning in a search for supersymmetry (SUSY) on the ATLAS experiment [53]. The signal data simulates the production of the supersymmetric χ^\pm which decays to W bosons and a supersymmetric χ^0 . The W 's then decay to charged leptons and neutrinos. Although the χ^0 and the neutrinos are not directly observable, their presence can be inferred from momentum imbalance and missing energy in the detector. The background events are a Standard Model process in which a pair of W bosons are produced and then each decay to a charged lepton and a neutrino, which is a commonly produced event at ATLAS with a signature that is similar to the signal events. BSW produced the event samples using Madgraph [54] and Pythia [55], and used Delphes [56] to simulate the response of

¹¹We verify the baseline MI value by processing the data through an ML algorithm, measuring MI on the output (I_f) using the histogram method, and comparing it to that baseline KSG measurement. I.e., we use the fact that I_f is trivial to compute and then confirm that $I_i = I_f$ as discussed in section 2.1.

¹²Because the added noise variables contain no information about the event classes, and are uncorrelated with any other variables, they each decrease the density of the variable space.

| # Noise | Standard KSG [bits] | T-KSG [bits] | Noise Included |
|---------|---------------------|--------------|----------------|
| 0 | 0.566(2) | 0.566(2) | n/a |
| 6 | 0.556(4) | 0.567(1) | 0 – 2 |
| 12 | 0.520(5) | 0.563(2) | 2 – 4 |
| 25 | 0.442(3) | 0.564(2) | 4 – 5 |
| 50 | 0.340(2) | 0.570(1) | 5 – 7 |
| 100 | 0.228(3) | 0.561(2) | 3 – 5 |

Table 1: **Gaussian Test.** MI calculations from standard KSG and our T-KSG method for a Gaussian dataset with a true MI of 0.566 ± 0.002 bits in the presence of varying amounts of noise. Column 1 shows the number of noise variables added to the data, column 2 shows that the MI estimate from standard KSG falls rapidly with increasing noise, column 3 shows the our estimate of MI is unaffected even by large amounts of noise, and column 4 shows how many of the noise variables were typically included by our algorithm. T-KSG typically took a 5-60 minutes for the tests with 0-50 added noise dimensions, and several hours for the test with 100 added noise dimensions. Details on the machine used for testing are given elsewhere 8.

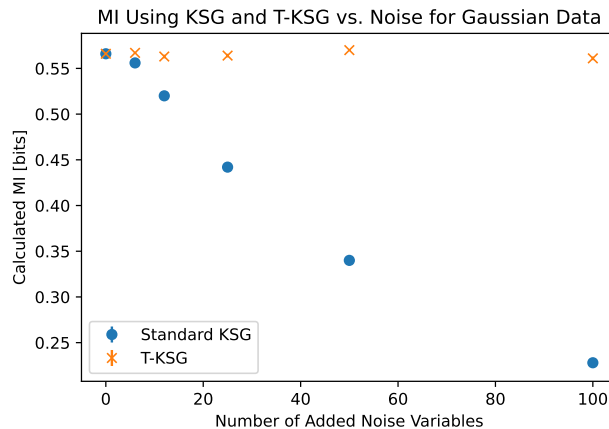


Figure 4: **Gaussian Test.** MI calculations from standard KSG and our T-KSG method for a Gaussian dataset with a true MI of 0.566 ± 0.002 bits in the presence of varying amounts of noise. This is the same data shown in Table 1. One sees clearly that our T-KSG estimate of MI remains stable and accurate even as noise and sparsity increase, while standard KSG begins to significantly underestimate MI as noise increases.

the ATLAS detector. The result is a signal dataset and a background dataset with 18 kinematic variables that mimic what one would see when searching the ATLAS data for production of this SUSY decay mode ¹³.

The details of the 18 kinematic events are not needed here, and are described elsewhere [17]. Briefly, there are eight variables that describe the momentum and angle of the two leptons along with the energy and momentum imbalance of the event. There are then ten additional variables that are functions of the first eight.

Searching for SUSY in the real data is a standard binary classification problem in which one first uses the distributions of the 18 variables in the simulated data to develop a model that distinguishes between the two event types and then applies that model to the real data. In practice, this often involves using an ML technique to create the model from the simulated data that discriminates between the event classes using the features in the signal and background datasets.

Our test of T-KSG on the SUSY data is functionally identical to the Gaussian test. We have two datasets which partially overlap and we want to estimate MI as a measure of how distinguishable, in principle, the signal is from the background. One difference between the two tests is that while every variable in the Gaussian study provides independent information about the class of an event, the SUSY data has, as described above, *primitive* variables (the first eight) and *derived* variables (the additional ten). Because the derived variables are simply functions of the primitive variables, they add no new information about which sample a given event is from. In a previous work [16], we found, as expected, that after

¹³Their datasets are publicly available [57]

Mutual Information in High Dimensions

calculating the amount of information that the primitive variables contained about event type, the derived variables did not add any new information. I.e., they did not increase KSG’s estimate of MI ¹⁴.

We will follow the same procedure to compare KSG with T-KSG that we used in the Gaussian study: We initially estimate MI using KSG and T-KSG on the dataset without adding any noise, and then add increasing amounts of noise to compare the stability of T-KSG to that of KSG.

Without noise, KSG and T-KSG give a consistent result of $(0.362 \pm 0.003 \text{ bits})$ as each other, and the same as the result found in Table 3 of [16] ¹⁵. The estimates from KSG and T-KSG as noise is added are shown in Table 2 and Figure 5. As in the Gaussian test, we see that as noise increases, KSG’s underestimate of MI worsens, while T-KSG’s estimate remains stable.

Column three of Table 2 shows that T-KSG typically includes ~ 2 noise variables. Although these don’t alter T-KSG’s estimate of MI, it is interesting to note that fewer noise variables are included in this test (~ 2) than were typically included in the Gaussian test (~ 4). As discussed in section 6.1, T-KSG is insensitive to additions of *small* numbers of noise variables, where *small* means few enough that KSG’s estimate of MI does not shift outside of statistical fluctuations and so doesn’t alter T-KSG’s choice of an optimum variable set. Comparing column 2 in Tables 1 and 2 shows that for the Gaussian data, standard KSG underestimates MI by only about 2% when 6 noise variables are added, while for the SUSY data, with the same amount of noise, the underestimate is 19%. This makes T-KSG more sensitive to added noise in the SUSY case and hence it will include fewer noise variables in its optimum set.

| # Noise | Standard KSG [bits] | T-KSG [bits] | Noise Included |
|---------|---------------------|--------------|----------------|
| 0 | 0.359(2) | 0.365(2) | n/a |
| 6 | 0.293(2) | 0.367(2) | 0 – 1 |
| 12 | 0.250(2) | 0.365(2) | 0 – 2 |
| 25 | 0.191(2) | 0.359(2) | 1 – 2 |
| 50 | 0.115(2) | 0.349(2) | 1 – 2 |
| 100 | 0.069(1) | 0.356(2) | 1 – 4 |

Table 2: **SUSY Test.** MI calculations from standard KSG and our T-KSG method for a SUSY dataset with a true MI of $0.362 \pm 0.003 \text{ bits}$ in the presence of varying amounts of noise. Column 1 shows the number of noise variables added to the data, column 2 shows that the MI estimate from standard KSG falls rapidly with increasing noise, column 3 shows the our estimate of MI is unaffected even by large amounts of noise, and column 4 shows how many of the noise variables were typically included by our algorithm. T-KSG typically took a 5-60 minutes for the tests with 0-50 added noise dimensions, and several hours for the test with 100 added noise dimensions. Details on the machine used for testing are given elsewhere 8.

7 Conclusion

MI is a centrally important quantitative measure of the correlations among variables. It is widely used in data analysis directly, and in studying models produced by ML algorithms. Despite its importance, existing methods for computing MI perform poorly in higher dimensions or in the presence of noise.

We presented our T-KSG method for accurately estimating MI even in higher dimensions and in the presence of noisy variables. T-KSG is a combination of the standard KSG method for measuring MI and the MCTS method that was developed to improve computers’ ability to play turn-based strategy games. To improve KSG, we developed a modified MCTS method that allows us to use a continuous result and to rapidly remove variables that would cause standard KSG to underestimate MI.

We have tested our method on a five-dimensional Gaussian sample and on an 18-dimensional sample of simulated SUSY data. For both studies, we verified that in the absence of noise, T-KSG and standard KSG give the same result as each other and the same result as an independent estimate of MI. We then added between 6 and 100 extra dimensions of noise and showed that T-KSG’s estimate of MI was stable while KSG’s estimate fell by 40 – 80%. Our software implementation of T-KSG is publicly available on GitHub.

¹⁴In [16] we actually used the Jensen-Shannon divergence between the signal and background samples as our metric rather than mutual information between the input data and the answer. However, for binary a classification problem the two quantities are the same.

¹⁵As in the Gaussian study, we verified this baseline value by processing the data through a neural network and measuring the MI of the one-dimensional output using a simple histogram method.

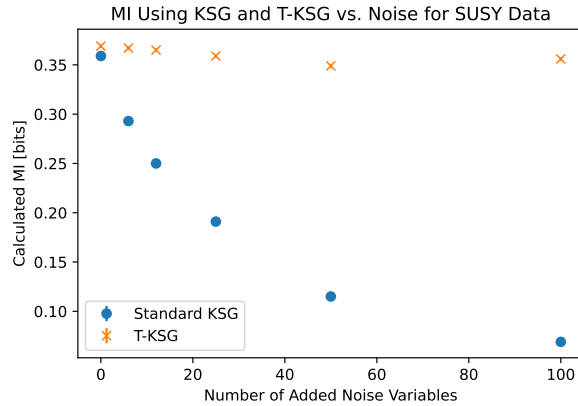


Figure 5: **SUSY Test.** MI calculations from standard KSG and our T-KSG method for a SUSY dataset with a true MI of 0.362 ± 0.003 bits in the presence of varying amounts of noise. This is the same data shown in Table 2. One sees clearly that our T-KSG estimate of MI remains stable and accurate even as noise and sparsity increase, while standard KSG begins to significantly underestimate MI as noise increases.

In addition to introducing the T-KSG method, we also reiterated discussions from a previous work on the importance of MI as: 1) an absolute measure of separability, 2) an absolute measure of an ML model’s performance, and 3) a way to rapidly carry out feature selection in high-dimensional data.

For convenience, we gather the most used terms and acronyms in Table 3.

| Term | Meaning |
|-------------------------|--|
| $\Delta_{\mathcal{T}}I$ | Our term for the absolute amount of information lost by a transformation (often an ML model). |
| DPI | Data Processing Inequality [1] |
| I_f | Our term for the MI between the output of a transformation (often an ML model) and the true classes of the events. |
| I_i | Our term for the MI between descriptive variables and the true classes of the events. |
| KL | An approach developed by L.F. Kozachenko and N.N. Leonenko for estimating the Shannon entropy of a continuous variable [41]. |
| KSG | The most widely used method for computing MI. Developed by Kraskov, Stögbauer, and Grassberger [18]. |
| MCTS | The Monte Carlo Tree Search method. |
| MI | Mutual Information |
| ML | Machine Learning |
| T-KSG | Our approach to computing MI, based on a combination of the KSG and MCTS methods. |

Table 3: Glossary of the most used terms and acronyms.

8 Acknowledgments

We thank Ariel Caticha and Greg Ver Steeg for helpful discussions. N.C. thanks the *Nuclear Science and Security Consortium* for research support.

This material is based upon work supported by the Department of Energy National Nuclear Security Administration through the Nuclear Science and Security Consortium under Award Number DE-NA0003996.

Disclaimer This report was prepared as an account of work sponsored by an agency of the United States Government. Neither the United States Government nor any agency thereof, nor any of their employees, makes any warranty, express of limited, or assumes any legal liability or responsibility for the accuracy, completeness, or usefulness of any information, apparatus, product, or process disclosed, or represents that its use would not infringe privately owned rights. Reference herein to any specific commercial product, process, or service by trade name, trademark, manufacturer, or

otherwise does not necessarily constitute or imply its endorsement, recommendation, or favoring by the United States Government or any agency thereof. The view and opinions of authors expressed herein do not necessarily state or reflect those of the United States Government or any agency thereof.

References

- [1] Thomas M Cover and Joy A Thomas. *Elements of Information Theory*. John Wiley & Sons, 2012.
- [2] D. Gencaga, N. K. Malakar, and D. J. Lary. Survey on the estimation of mutual information methods as a measure of dependency versus correlation analysis. *arXiv*, page 1401.3358v1, 2014.
- [3] Isabelle Guyon and André Elisseeff. An introduction to variable and feature selection. *J. Mach. Learn. Res.*, 3:1157–1182, 2003.
- [4] V. Sindhwani, S. Rakshit, D. Deodhare, D. Erdogmus, J.C. Principe, and P. Niyogi. Feature selection in mlps and svms based on maximum output information. *IEEE Transactions on Neural Networks*, 15(4):937–948, 2004.
- [5] Peng Hanchuan, Long Fuhui, and C. Ding. Feature selection based on mutual information criteria of max-dependency, max-relevance, and min-redundancy. *IEEE Transactions on Pattern Analysis and Machine Intelligence*, 27(8):1226–1238, 2005.
- [6] Roberto Battiti. Using mutual information for selecting features in supervised neural net learning. *Neural Networks, IEEE Transactions on*, 5:537 – 550, 1994.
- [7] Boyan Bonev, Francisco Escolano, and Miguel Cazorla. Feature selection, mutual information, and the classification of high-dimensional patterns. *Pattern Analysis and Applications*, 11(3):309–319, 2008.
- [8] Ralph Linsker. Self-organization in a perceptual network. *IEEE Computer*, 21:105–117, 1988.
- [9] R. Vergara Jorge and A. Estévez Pablo. A review of feature selection methods based on mutual information. *Neural Computing and Applications*, 24(1):175–186, 2013.
- [10] Arnab Mondal, Arnab Bhattacharjee, Sudipto Mukherjee, Himanshu Asnani, Sreeram Kannan, and Prathosh A P. C-mi-gan : Estimation of conditional mutual information using minmax formulation proceedings of the 36th conference on uncertainty in artificial intelligence (uai). *Proceedings of Machine Learning Research*, 124:849–858, 2020.
- [11] Pablo A. Estevez, Michel Tesmer, Claudio A. Perez, and Jacek M. Zurada. Normalized mutual information feature selection. *IEEE Transactions on Neural Networks*, 20(2):189–201, 2009.
- [12] Ver Steeg Greg and Galstyan Aram. *The Information Sieve*. 2016.
- [13] Foithong Sombut, Pinnern Ouen, and Attachoo Boonwat. Feature subset selection wrapper based on mutual information and rough sets. *Expert Systems with Applications*, 39(1):574–584, 2012.
- [14] Kari Torkkola. Feature extraction by non parametric mutual information maximization. *J. Mach. Learn. Res.*, 3:1415–1438, 2003.
- [15] Francois Fleuret. Fast binary feature selection with conditional mutual information. *J. Mach. Learn. Res.*, 5:1531–1555, 2004.
- [16] Nicholas Carrara and Jesse A. Ernst. On the upper limit of separability. 2017.
- [17] P. Baldi, P. Sadowski, and D. Whiteson. Searching for exotic particles in high-energy physics with deep learning. *Nature Communications*, 5(1):4308, 2014.
- [18] Alexander Kraskov, Harald Stögbauer, and Peter Grassberger. Estimating mutual information. *Physical Review E*, 69(6), 2004.
- [19] Shuyang Gao, Greg Ver Steeg, and Aram Galstyan. Efficient estimation of mutual information for strongly dependent variables. *arXiv*, page 1411.2003v3, 2014.
- [20] Shuyang Gao, Greg Ver Steeg, and Aram Galstyan. Estimating mutual information by local gaussian approximation. *arXiv*, page 1508.00536v2, 2015.
- [21] Shashank Singh and Barnabás Póczos. Analysis of k-nearest neighbor distances with application to entropy estimation. *arXiv*, page 1603.08578v2, 2016.
- [22] Czyż Paweł, Grabowski Frederic, E. Vogt Julia, Beerenwinkel Niko, and Marx Alexander. *Beyond Normal: On the Evaluation of Mutual Information Estimators*. 2023.

- [23] Cameron B Browne, Edward Powley, Daniel Whitehouse, Simon M Lucas, Peter I Cowling, Philipp Rohlfshagen, Stephen Tavener, Diego Perez, Spyridon Samothrakis, and Simon Colton. A survey of monte carlo tree search methods. *IEEE Transactions on Computational Intelligence and AI in games*, 4(1):1–43, 2012.
- [24] D Silver, A Huang, CJ Maddison, A Guez, L Sifre, G van den Driessche, J Schrittwieser, I Antonoglou, V Panneershelvam, M Lanctot, S Dieleman, D Grewe, J Nham, N Kalchbrenner, I Sutskever, T Lillicrap, M Leach, K Kavukcuoglu, T Graepel, and D Hassabis. Mastering the game of go with deep neural networks and tree search. *Nature*, 529(7587):484–489, 2016.
- [25] Piras Davide, V Peiris Hiranya, Pontzen Andrew, Lucie-Smith Luisa, Guo Ningyuan, and Nord Brian. A robust estimator of mutual information for deep learning interpretability. *Machine Learning: Science and Technology*, 4(2):025006, 2023.
- [26] R Devon Hjelm, Alex Fedorov, Samuel Lavoie-Marchildon, Karan Grewal, Phil Bachman, Adam Trischler, and Yoshua Bengio. Learning deep representations by mutual information estimation and maximization. 2018.
- [27] Grabowski Frederic, Czyż Paweł, Kochańczyk Marek, and Lipniacki Tomasz. *Limits to the rate of information transmission through MAPK pathway*. Cold Spring Harbor Laboratory, 2018.
- [28] Li Bo, Shen Yifei, Wang Yezhen, Zhu Wenzhen, J. Reed Colorado, Zhang Jun, Li Dongsheng, Keutzer Kurt, and Zhao Han. *Invariant Information Bottleneck for Domain Generalization*. 2022.
- [29] C. E. Shannon. A mathematical theory of communication. *The Bell System Technical Journal*, 27(3):379–423, 1948.
- [30] G Doquire and M Verleysen. A comparison of multivariate mutual information estimators for feature selection. *ICPRAM (1)*, 2012.
- [31] Bennasar Mohamed, Hicks Yulia, and Setchi Rossitza. Feature selection using joint mutual information maximization. *Expert Systems with Applications*, 42(22):8520–8532, 2015.
- [32] Ralph Linsker. Neural information processing systems towards an organizing principle for a layered perceptual network. 0, 1988.
- [33] Anthony J. Bell and Terrence J. Sejnowski. An information-maximization approach to blind separation and blind deconvolution. *Neural Computation*, 7(6):1129–1159, 1995.
- [34] Ming-Jie Zhao, Narayanan Edakunni, Adam Pocock, and Gavin Brown. Beyond fano’s inequality: Bounds on the optimal f-score, ber, and cost-sensitive risk and their implications. *J. Mach. Learn. Res.*, 14(1):1033–1090, 2013.
- [35] Jonathan Scarlett and Volkan Cevher. An introductory guide to fano’s inequality with applications in statistical estimation. 2019.
- [36] M. Hellman and J. Raviv. Probability of error, equivocation, and the chernoff bound. *IEEE Transactions on Information Theory*, 16(4):368–372, 1970.
- [37] Roberts S. and Evernson (Eds. R. *Independent Component Analysis: Principles and Practice*. Cambridge University Press, 2001.
- [38] J. Karhunen A. Hyvarinen and Oja E. *Independent Component Analysis*. Wiley, New York, 2001.
- [39] M. Holmes Caroline and Nemenman Ilya. Estimation of mutual information for real-valued data with error bars and controlled bias. *Physical Review E*, 100(2), 2019.
- [40] Liam Paninski. Estimation of entropy and mutual information. *Neural Computation*, 15(6):1191–1253, 2003.
- [41] LF Kozachenko and NN Leonenko. Sample estimate of the entropy of a random vector. *Problemy Peredachi Informatsii*, 25:95, 1987.
- [42] Alexander Marx and Jonas Fischer. Estimating mutual information via geodesic k nn. *arXiv*, page 2110.13883v2, 2021.
- [43] Nicholas Carrara and Kevin Vanslette. The design of global correlation quantifiers and continuous notions of statistical sufficiency. *Entropy*, 22(3), 2020.
- [44] Nicholas Carrara and Jesse Ernst. On the estimation of mutual information. *The 39th International Workshop on Bayesian Inference and Maximum Entropy Methods in Science and Engineering*, 2020.
- [45] Weihao Gao, Sewoong Oh, and Pramod Viswanath. Density functional estimators with k -nearest neighbor bandwidths. *2017 IEEE International Symposium on Information Theory (ISIT)*, pages 1351–1355, 2017.
- [46] E.M. Bollt W.M. Lord, J. Sun. Geometric k -nearest neighbor estimation of entropy and mutual information. *Chaos: An Interdisciplinary Journal of Nonlinear Science*, 28(3), 2018.

- [47] Levente Kocsis and Csaba Szepesvári. Bandit based monte-carlo planning. *Machine Learning: ECML*, 2006:282–293, 2006.
- [48] G. Reddy, A. Celani, and Vergassola M. Infomax strategies for an optimal balance between exploration and exploitation. *Journal of Statistical Physics*, 163(6):1454–1476, 016 apr.
- [49] Lai T.L and Robbins Herbert. Asymptotically efficient adaptive allocation rules. *Advances in Applied Mathematics*, 6(1):4–22, 1985.
- [50] N. Carrara. The foundations of inference and its application to fundamental physics. *Ph.D. Thesis*.
- [51] Romaric Gaudel and Michele Sebag. Feature selection as a one-player game proceedings of the 27th international conference on international conference on machine learning. *ICML'10*, pages 359–366, 2010.
- [52] Muhammad Umar Chaudhry and Jee-Hyong Lee. Feature selection for high dimensional data using monte carlo tree search. *IEEE Access*, 6:76036–76048, 2018.
- [53] ATLAS Collaboration The. The atlas experiment at the cern large hadron collider. *Journal of Instrumentation*, 3(08):S08003, 2008.
- [54] Johan Alwall, Michel Herquet, Fabio Maltoni, Olivier Mattelaer, and Tim Stelzer. Madgraph 5: going beyond. *Journal of High Energy Physics*, 2011(6):128, 2011.
- [55] Sjöstrand Torbjörn, Mrenna Stephen, and Skands Peter. Pythia 6.4 physics and manual. *Journal of High Energy Physics*, 2006(05):026–026, 2006.
- [56] Séverine Ovin, Xavier Rouby, and Vincent Lemaitre. Delphes, a framework for fast simulation of a generic collider experiment. *arXiv preprint arXiv:0903.2225*, 2009.
- [57] Dheeru Dua and Casey Graff. UCI machine learning repository. 2017.